



HAL
open science

Electron removal energies in noble-gas atoms up to 100 keV: Ab initio GW versus x-ray photoelectron spectroscopy

Iskander Mukatayev, Benoît Sklénard, Valerio Olevano, Jing Li

► **To cite this version:**

Iskander Mukatayev, Benoît Sklénard, Valerio Olevano, Jing Li. Electron removal energies in noble-gas atoms up to 100 keV: Ab initio GW versus x-ray photoelectron spectroscopy. *Physical Review B*, 2022, 106 (8), pp.L081125. 10.1103/PhysRevB.106.L081125 . hal-03629879

HAL Id: hal-03629879


<https://hal.science/hal-03629879>

Submitted on 11 Aug 2023

HAL is a multi-disciplinary open access archive for the deposit and dissemination of scientific research documents, whether they are published or not. The documents may come from teaching and research institutions in France or abroad, or from public or private research centers.

L'archive ouverte pluridisciplinaire **HAL**, est destinée au dépôt et à la diffusion de documents scientifiques de niveau recherche, publiés ou non, émanant des établissements d'enseignement et de recherche français ou étrangers, des laboratoires publics ou privés.

Electron removal energies in noble-gas atoms up to 100 keV: *Ab initio* GW versus x-ray photoelectron spectroscopy

Iskander Mukatayev,¹ Benoît Sklénard ^{1,2} Valerio Olevano,^{3,4,2,*} and Jing Li^{1,2,†}

¹Université Grenoble Alpes, CEA, Leti, F-38000 Grenoble, France

²European Theoretical Spectroscopy Facility (ETSF), F-38000 Grenoble, France

³Université Grenoble Alpes, F-38000 Grenoble, France

⁴CNRS, Institut Néel, F-38042 Grenoble, France



(Received 18 March 2022; revised 5 July 2022; accepted 12 July 2022; published 29 August 2022)

X-ray photoelectron spectroscopy (XPS) measures electron removal energies, providing direct access to core and valence electron binding energies, hence probing the electronic structure. In this Letter, we benchmark the *ab initio* many-body *GW* approximation on the complete electron binding energies of noble-gas atoms (He-Rn), which span 100 keV. Our results demonstrate that *GW* achieves an accuracy within 1.2% in XPS binding energies, by systematically restoring the underestimation from density-functional theory (error of 14%) or the overestimation from Hartree-Fock (error of 4.7%). Such results also imply the correlations of *d* electrons are very well described by *GW*.

DOI: [10.1103/PhysRevB.106.L081125](https://doi.org/10.1103/PhysRevB.106.L081125)

Introduction. The electronic structure of atoms, molecules, and solids [1] is characterized by neutral excitations, as measured in optical spectroscopy, and charged electron removal/addition excitations, as measured in direct/inverse photoemission spectroscopy. In x-ray photoelectron spectroscopy (XPS) [2,3] an x-ray photon of fixed energy interacts with the electronic structure and removes an electron that escapes from the system with accurately measurable kinetic energy. The difference between the energy of the primary photon and the kinetic energy of the emitted electron provides the removal energy which coincides with the binding energy (BE) of the electron into the system. XPS was established as one of the most powerful techniques to access the electronic structure and charged excitations. Binding energies of electrons in occupied states, either core or valence, can be measured with an accuracy of up to 10^{-3} eV by XPS.

From a theoretical point of view, the calculation of electron removal/addition energies is challenging [1,4]. An exact analytic solution of the Schrödinger equation for electron BEs is only available for one-electron systems, e.g., the hydrogen atom. Already in helium one should take into account an electron-electron interaction term in the Hamiltonian which faces a many-body problem [5,6]. The simplest and historically the first way to tackle this problem is by mean-field approaches, e.g., the Hartree or the Hartree-Fock methods, in which the interaction of one electron with all other electrons is replaced by a mean-field potential self-consistently calculated. In Hartree-Fock (HF) the Koopmans' theorem holds and states that HF eigenvalues are directly associated with electron removal/addition energies [1,4]. However, the HF is an approximated method that neglects correlation energies. On

valence and core electron levels, this reflects in a systematic overestimation of BEs, as we will show.

Today, a more popular approach to tackle the many-body problem is density-functional theory (DFT) [7–10]. DFT is an in-principle exact approach to calculate the total ground-state energy. In DFT, electron removal/addition energies can be calculated by the so-called Delta self-consistent field (Δ SCF) method [9,10] as the total energy differences between the neutral and ionized systems. However, the Δ SCF method is exact only when calculating the highest occupied molecular orbital (HOMO) and the lowest unoccupied (LUMO) binding energies, that is, the ionization potential (IP) and the electron affinity (EA). It can be justified for the lowest levels within a given symmetry [11]. For other levels, assumptions must be imposed on the relaxation of the ion, e.g., the localization of the core hole, leading to inaccuracy. Furthermore, the Δ SCF method can in principle be applied only to finite systems [9,10]. In periodic solids some other assumptions/corrections, such as adding an infinite compensating charge on the background, are required, leading again to inaccuracies. Nevertheless, even in approximated DFT, such as in local-density approximation (LDA) or beyond [Perdew-Burke-Ernzerhof (PBE)] [12,13], the Δ SCF method generally compares well with the experiment. For the lightest elements deviations typically lie in the range 0.3–0.7 eV [14], but can increase by one order of magnitude [15].

In DFT, Kohn-Sham (KS) eigenvalues are very often directly used to estimate electron removal/addition energies [9,10]. This procedure is in principle exact only to evaluate the IP equal to the last occupied KS energy [16–18]. Indeed, the Koopmans' theorem does not hold in DFT as in HF. A physical interpretation of the other DFT KS eigenvalues as electron removal/addition energies, such as HF eigenvalues, would imply that DFT, as HF, is a mean-field theory. But the DFT exchange-correlation (xc) potential $v_{xc}(r)$ of the fictitious KS system is not constructed as a mean-field

*valerio.olevano@neel.cnrs.fr

†jing.li@cea.fr

approximation of the true self-energy, as is the case for the HF exchange operator. To this error of principle, we must further add the error due to the unavoidable approximation on the xc functional of DFT. As we will show, DFT KS energies in the PBE (or LDA) approximations systematically underestimate the core and valence electron BEs, with an error that is larger than HF for finite systems.

In this Letter, we calculate the electron binding energies of noble-gas atoms within the framework of many-body perturbation theory (MBPT) and using the *GW* approximation on the self-energy [19–23]. MBPT or Green’s function theory is an in-principle exact framework to calculate electron removal/addition energies which directly correspond to the poles of the one-particle Green’s function [4]. The Green’s function can be calculated via the Dyson equation from the self-energy [4], but the exact form of the latter is too complex for real systems. Although in principle exact, MBPT must also resort to approximations. The *GW* approximation to the MBPT self-energy has demonstrated its validity on the band gaps of solids [1,24], and of the HOMO-LUMO gaps of molecules [25–27]. Here, we benchmark *GW* on the core levels of atoms. In particular, we choose noble-gas atoms because they are closed shell and electron energy levels are unaffected by other complications, such as chemical shifts due to the molecular or solid-state environment. Previous *GW* calculations on atoms [28–30] only studied valence electrons. There are some *GW* attempts to study at least shallow core states in solids [31,32] and molecules [15,33–35]. Here, the *GW* approximation is tested at energies as deep as 100 keV.

Methods. The starting point of our *ab initio* procedure is a standard HF, or alternatively a DFT-PBE calculation. Relativistic effects are evaluated by the zero-order regular approximation (ZORA) [36–38] and also the third-order Douglas-Kroll (DK3) approximation [39,40]. Their respective performances have been assessed with respect to experimental atomic spin-orbit (SO) splits which can be measured accurately without calibration problems such as, for example, the systematic rigid energy shift due to the sample charging drawback of photoemission. Table I presents SO splits in the DK3 and ZORA approximations on top of both DFT-PBE and HF, together with their overall mean absolute error (MAE in eV) and mean absolute percentage error (MAPE) with respect to the experiment. In noble-gas atoms the ZORA is more accurate than the DK3. Unless differently specified, in the following we will only present and discuss ZORA results. In any case, *GW* corrections depend weakly from the relativistic approximation [41].

DFT KS or HF eigenvalues E_i and eigenfunctions ϕ_i are then used to build the first-iteration Green’s function,

$$G(r, r', \omega) = \sum_i \frac{\phi(r)\phi_i^*(r')}{\omega - E_i - i\eta \operatorname{sgn}(\mu - E_i)}, \quad (1)$$

with μ the chemical potential and η a positive infinitesimal. From G we build the random-phase approximation (RPA) polarizability, $\Pi = -iGG$, and the screened Coulomb potential $W = w + w\Pi W$ (with $w = 1/|r - r'|$ the bare Coulomb potential), and finally the self-energy in the *GW* approximation,

$$\Sigma(r, r', \omega) = \frac{i}{2\pi} \int d\omega' e^{i\omega'\eta} G(r, r', \omega + \omega') W(r, r', \omega'),$$

TABLE I. He to Xe spin-orbit (SO) split in the DK3 and ZORA relativistic approximations on top of DFT-PBE and HF, and their overall mean absolute error (MAE) and mean absolute percentage error (MAPE) with respect to the experiment (XPS of Ref. [2], except Ne 2*p*, Ar 3*p*, Kr 4*p*, and Xe 4*p*_{1/2} which are from Ref. [42]).

SO split (eV)		DK3		ZORA		Expt.
Atom	Orbit	PBE	HF	PBE	HF	
Ne	2 <i>p</i>	0.06	0.08	0.10	0.13	0.10
Ar	2 <i>p</i>	1.22	1.32	2.17	2.34	2.11
	3 <i>p</i>	0.10	0.12	0.17	0.21	0.18
Kr	2 <i>p</i>	27.9	28.6	52.9	54.3	52.5
	3 <i>p</i>	4.1	4.4	7.8	8.4	7.8
	3 <i>d</i>	0.9	0.9	1.3	1.4	1.2
	4 <i>p</i>	0.33	0.39	0.62	0.73	0.67
Xe	2 <i>p</i>	163.1	165.8	322.5	327.6	319.9
	3 <i>p</i>	31.1	32.4	61.2	63.9	61.5
	3 <i>d</i>	7.8	8.1	12.9	13.4	12.6
	4 <i>p</i>	6.2	6.5	12.2	12.8	11.5
	4 <i>d</i>	1.2	1.3	2.0	2.1	2.0
	5 <i>p</i>	0.62	0.73	1.22	1.43	1.27
MAE		17.6	17.1	0.35	1.18	
MAPE		44.2%	38.4%	3.1%	10.0%	

where the ω' integral is carried on by contour deformation and we did not carry an analytic continuation on Σ which would lead to large errors on the deep core states. The *GW* charged excitation quasiparticle energies are calculated by

$$E_i^{GW} = E_i^H + \langle \phi_i | \Sigma(\omega = E_i^{GW}) | \phi_i \rangle, \quad (2)$$

where the E_i^H are the Hartree energies, i.e., the eigenvalues of the Hamiltonian only containing kinetic, nucleus external potential, and Hartree classical repulsion terms. The procedure can stop here to get the first iteration G^0W^0 energies, or a self-consistency can be carried on by recalculating G in Eq. (1) with the new energies Eq. (2) (eigenvalue self-consistency). Then the new G can be used to recalculate directly only Σ (ev*GW*⁰ self-consistency), or also Π and so W (ev*GW*). In our work we used ev*GW*, but both flavors reduce the dependence from the starting point [43], although more complete self-consistency would require us to recalculate also the wave functions, and even the full G , i.e., including the noncoherent part. All the calculations were performed using Gaussian basis sets. To access the deep core states and their relativistic effect, we used x2c-TZVPPall-2c [44] segmented contracted Gaussian basis sets optimized at the one-electron exact two-component level. Also, a Coulomb-fitting resolution of the identity technique (RI-V) [45] is employed with the auxiliary basis def2-universal-JKFIT [46] for He-Kr and the auxiliary basis generated by AUTOAUX [47] for Xe and Rn. We used the codes NWCHEM [48] for the HF and DFT calculations, and FIESTA [49–51] with some checks by TURBOMOLE [52] for *GW*.

Results. Figure 1 shows the relative magnitude of *GW* many-body and ZORA scalar relativistic (SR) corrections to the HF and DFT-PBE energies of the 1*s* level as a function of the atomic number Z . ZORA scalar relativistic corrections do not depend on whether they are applied on top of PBE or

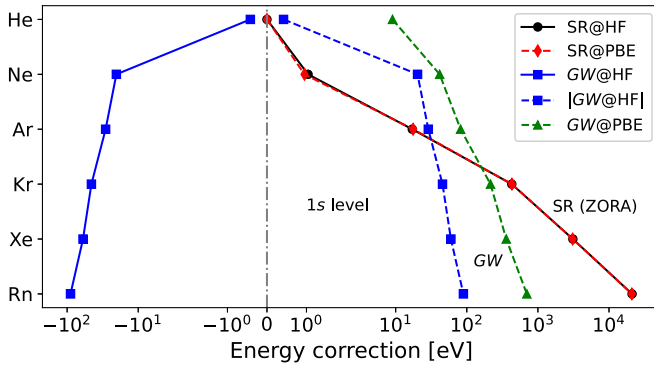


FIG. 1. *GW* vs ZORA scalar relativistic (SR) corrections to the PBE and HF energies of the $1s$ level of noble-gas atoms.

HF, since the two curves overlap (same for DK3 [41]). They undergo a large increase with Z , going beyond 3 keV in Xe (20 keV in Rn). In contrast, *GW* corrections on top of HF have small negative values, not going beyond -100 eV, to reduce the slight overestimation of HF energies. On the other hand, *GW* corrections on top of PBE have a large increase with Z , so to reduce the large underestimation of PBE energies. *GW* corrections are larger than SR at small Z , and become smaller at large Z , although still not negligible (360 eV correction at Xe, 700 eV for Rn). They can never be neglected.

Figure 2 shows the error with respect to the experiment on the electronic binding energies calculated within the ZORA relativistic scheme in all exchange-correlation approximations. Overall MAE and MAPE are presented in Table II and full detailed results on the electronic binding energies in Table III [41]. As experimental reference values we have taken the XPS binding energies reported in Ref. [2], except for Ne $2p$, Ar $3p$, Kr $1s$ and $4p$, Xe $1s$ and $4p_{1/2}$, and Rn which are taken from Ref. [42]. We consider the former more direct and

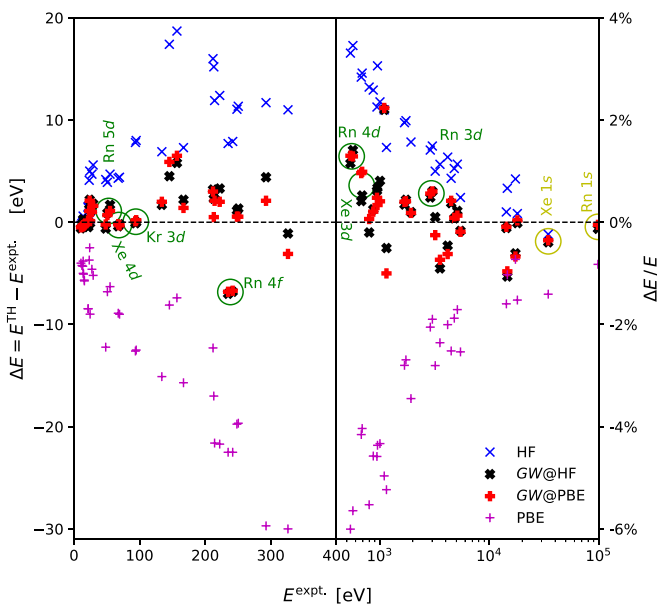


FIG. 2. Noble-gas atoms' ZORA PBE, HF, and *GW* electronic energy absolute (left, 0–400 eV) and relative (right, from 400 eV to 10^5 eV) errors with respect to the experiment [2,42].

TABLE II. Noble-gas atoms (He to Xe) electronic binding energies in the DFT-PBE, HF, *GW* (on top of PBE and HF), ZORA, and DK3 approximations: mean absolute error (MAE in eV) and mean absolute percentage error (MAPE) with respect to the experiment.

BE (binding energies)	MAE		MAPE	
	ZORA	DK3	ZORA	DK3
PBE	44.5	39.9	14.0%	14.1%
HF	16.2	20.6	4.7%	4.8%
<i>GW</i> @PBE	6.0	10.4	1.2%	1.4%
<i>GW</i> @HF	6.3	10.0	1.2%	1.4%

accurate, but values from the latter are not far when both are available. In any case, our conclusions do not change if we use the similar values of Refs. [3,53,54] (see also Ref. [55]).

As we already anticipated in the Introduction, we can see from Fig. 2 and Table III that DFT-PBE KS energies systematically underestimate experimental BEs. The underestimation can be as large as 500 eV in Xe $1s$ and 800 eV in Rn $1s$. However, since the Xe $1s$ level is already 34.5 keV deep, the relative error is only 1.4%. Starting from the deepest levels, the PBE underestimation relative error systematically increases, so to achieve almost 40% in the shallowest levels. This error precisely corresponds to the DFT-PBE (or LDA) systematic underestimation of the HOMO-LUMO gap for finite systems, and of the band gap in infinite periodic solids. On the other hand, in general, HF eigenvalues overestimate removal energies, though less systematically (for instance, Xe and Rn $1s$ levels are underestimated). However the HF error is smaller. We can conclude that HF is better than DFT-PBE on noble-gas atoms at all binding energies.

In Fig. 2, we then immediately remark on the net improvement brought by *GW* calculations, both on top of PBE and HF (*GW*@PBE and *GW*@HF, respectively). First note that our data are not the results of a single iteration G^0W^0 calculation, but we have performed a self-consistency on the quasiparticle energies only, whereas wave functions have been kept at their iteration 0 level, that is, PBE or HF wave functions. So, regardless of the starting point, self-consistent *GW* energies surprisingly achieve almost the same value. *GW*@PBE and *GW*@HF are distant by only a few tenths of an eV on the shallowest energies and a few tenths of a percentage on the deepest energies. *GW* self-consistency on energies only is then sufficient to get a result that is almost independent on the starting point. Also, PBE and HF are among the most distant starting points, in practice, the two extremes in hybrid theories [56]. Our data indicate that PBE and HF wave functions are very close for noble-gas atoms, with the main difference being in energies.

For a fair evaluation of the validity of the *GW* approximation with respect to the experiment, we believe that a correct interpretation should take into account from one side the absolute error, $\Delta E = E^{\text{TH}} - E^{\text{expt.}}$, for the shallowest levels, as it is done in the left part from 0 to 400 eV of Fig. 2; and from another side, the relative error, $\Delta E/E^{\text{expt.}}$, for the lowest-lying core levels which are placed thousands of eV deep, as it is done in the right part of Fig. 2 from 400 eV to 100 keV. Indeed, the 0.1–0.2 eV accuracy achieved by *GW* on low-energy

TABLE III. ZORA electron binding energies (eV) and errors with respect to the experiment (Ref. [2], except [†] from Ref. [42]).

Atom	Orbital	PBE: E	ΔE	$\Delta E/E$	GW@PBE: E	ΔE	$\Delta E/E$	Expt.: E	GW@HF: E	ΔE	$\Delta E/E$	HF: E	ΔE	$\Delta E/E$
He	1s	15.6	-9.0	-36.4%	24.7	0.1	0.3%	24.59	24.5	-0.1	-0.2%	24.9	0.4	1.5%
Ne	1s	830.4	-39.8	-4.6%	872.0	1.8	0.2%	870.2	872.4	2.2	0.3%	892.7	22.5	2.6%
	2s	36.2	-12.2	-25.3%	48.2	-0.2	-0.5%	48.42	47.8	-0.6	-1.3%	52.6	4.2	8.6%
	2p _{1/2}	13.2	-8.5	-39.1%	21.8	0.1	0.4%	†21.66	21.2	-0.4	-1.9%	23.2	1.5	7.0%
Ar	2p _{3/2}	13.1	-8.5	-39.2%	21.7	0.1	0.4%	†21.56	21.1	-0.4	-2.1%	23.0	1.5	6.9%
	1s	3116.0	-89.9	-2.8%	3197.8	-8.1	-0.3%	3205.9	3209.1	3.2	0.1%	3237.9	31.9	1.0%
	2s	296.3	-30.0	-9.2%	323.2	-3.1	-0.9%	326.3	325.2	-1.1	-0.3%	337.3	11.0	3.4%
Kr	2p _{1/2}	230.9	-19.7	-7.8%	251.1	0.6	0.2%	250.56	251.9	1.4	0.5%	261.9	11.3	4.5%
	2p _{3/2}	228.7	-19.7	-7.9%	249.0	0.5	0.2%	248.45	249.6	1.1	0.5%	259.5	11.1	4.5%
	3s	24.1	-5.2	-17.7%	30.9	1.6	5.5%	29.3	31.1	1.8	6.1%	34.9	5.6	19.3%
Xe	3p _{1/2}	10.2	-5.7	-35.8%	15.7	-0.3	-1.6%	†15.94	15.8	-0.1	-0.9%	16.2	0.2	1.4%
	3p _{3/2}	10.1	-5.7	-36.1%	15.5	-0.2	-1.5%	†15.76	15.6	-0.2	-1.1%	16.0	0.2	1.2%
	1s	14098.2	-228.8	-1.6%	14314.3	-12.7	-0.1%	†14327	14310.9	-16.1	-0.1%	14355.9	28.9	0.2%
Rn	2s	1858.2	-66.4	-3.4%	1928.1	3.5	0.2%	1924.6	1928.4	3.8	0.2%	1954.8	30.2	1.6%
	2p _{1/2}	1684.3	-46.6	-2.7%	1738.0	7.1	0.4%	1730.9	1738.5	7.6	0.4%	1765.3	34.4	2.0%
	2p _{3/2}	1631.4	-47.0	-2.8%	1685.1	6.7	0.4%	1678.4	1684.2	5.8	0.3%	1711.1	32.7	1.9%
He	3s	263.1	-29.7	-10.1%	294.9	2.1	0.7%	292.8	297.2	4.4	1.5%	304.5	11.7	4.0%
	3p _{1/2}	200.5	-21.7	-9.8%	224.2	2.0	0.9%	222.2	225.5	3.3	1.5%	234.6	12.4	5.6%
	3p _{3/2}	192.8	-21.6	-10.1%	216.5	2.1	1.0%	214.4	217.1	2.7	1.3%	226.3	11.9	5.5%
Ne	3d _{3/2}	82.4	-12.5	-13.2%	95.1	0.2	0.2%	94.9	94.9	0.0	0.0%	102.9	8.0	8.4%
	3d _{5/2}	81.1	-12.6	-13.4%	93.8	0.1	0.1%	93.7	93.6	-0.1	-0.2%	101.5	7.8	8.4%
	4s	22.8	-4.6	-16.7%	28.4	1.0	3.7%	27.4	28.6	1.2	4.5%	32.1	4.7	17.3%
Ar	4p _{1/2}	9.6	-5.0	-34.4%	14.3	-0.4	-2.5%	†14.67	14.4	-0.3	-1.7%	14.7	0.1	0.4%
	4p _{3/2}	9.0	-5.0	-35.7%	13.7	-0.3	-2.3%	†14	13.7	-0.3	-2.2%	14.0	0.0	-0.1%
	1s	34078.5	-486.5	-1.4%	34443.0	-122.0	-0.4%	†34565	34429.0	-136.0	-0.4%	34483.5	-81.5	-0.2%
Kr	2s	5314.9	-138.3	-2.5%	5443.0	-10.2	-0.2%	5453.2	5444.0	-9.2	-0.2%	5479.6	26.4	0.5%
	2p _{1/2}	5019.9	-87.3	-1.7%	5113.8	6.6	0.1%	5107.2	5118.5	11.3	0.2%	5165.2	58.0	1.1%
	2p _{3/2}	4697.4	-89.9	-1.9%	4791.4	4.1	0.1%	4787.3	4790.9	3.6	0.1%	4837.6	50.3	1.1%
Xe	3s	1088.6	-60.1	-5.2%	1137.2	-11.5	-1.0%	1148.7	1142.9	-5.8	-0.5%	1165.5	16.8	1.5%
	3p _{1/2}	958.7	-43.4	-4.3%	1006.2	4.1	0.4%	1002.1	1010.2	8.1	0.8%	1025.7	23.6	2.4%
	3p _{3/2}	897.5	-43.1	-4.6%	945.1	4.5	0.5%	940.6	946.4	5.8	0.6%	961.8	21.2	2.3%
Rn	3d _{3/2}	661.2	-27.8	-4.0%	695.8	6.8	1.0%	689	692.6	3.6	0.5%	709.1	20.1	2.9%
	3d _{5/2}	648.3	-28.1	-4.2%	682.9	6.5	1.0%	676.4	679.2	2.8	0.4%	695.6	19.2	2.8%
	4s	196.2	-17.0	-8.0%	213.7	0.5	0.2%	213.2	215.5	2.3	1.1%	228.4	15.2	7.1%
He	4p _{1/2}	149.6	-7.4	-4.7%	163.5	6.5	4.2%	†157	162.8	5.8	3.7%	175.7	18.7	11.9%
	4p _{3/2}	137.4	-8.1	-5.5%	151.4	5.9	4.0%	145.5	150.0	4.5	3.1%	162.9	17.4	11.9%
	4d _{3/2}	60.5	-9.0	-12.9%	69.2	-0.3	-0.4%	69.5	69.3	-0.2	-0.3%	73.9	4.4	6.3%
Ne	4d _{5/2}	58.6	-8.9	-13.2%	67.3	-0.2	-0.4%	67.5	67.1	-0.4	-0.5%	71.8	4.3	6.3%
	5s	19.6	-3.7	-16.0%	24.4	1.1	4.7%	23.3	24.6	1.3	5.7%	27.4	4.1	17.6%
	5p _{1/2}	9.1	-4.3	-32.3%	13.0	-0.4	-3.2%	13.4	13.3	-0.1	-0.7%	13.4	0.0	0.3%
Ar	5p _{3/2}	7.9	-4.3	-35.3%	11.7	-0.4	-3.2%	12.13	11.9	-0.3	-2.1%	12.0	-0.1	-1.0%
	1s	97593.1	-810.9	-0.8%	98353.6	-50.4	-0.1%	†98404	98276.9	-127.1	-0.1%	98308.1	-95.9	-0.1%
	2s	17780.2	-274.8	-1.5%	18061.5	6.5	0.0%	†18055	18051.8	-3.2	0.0%	18085.7	30.7	0.2%
Kr	2p _{1/2}	17207.9	-126.1	-0.7%	17217.7	-116.3	-0.7%	†17334	17228.4	-105.6	-0.6%	17480.7	146.7	0.8%
	2p _{3/2}	14464.8	-150.2	-1.0%	14474.6	-140.4	-1.0%	†14615	14459.8	-155.2	-1.1%	14712.0	97.0	0.7%
	3s	4370.1	-112.9	-2.5%	4501.8	18.8	0.4%	†4483	4499.7	16.7	0.4%	4521.5	38.5	0.9%
Xe	3p _{1/2}	4078.6	-83.4	-2.0%	4136.1	-25.9	-0.6%	†4162	4142.9	-19.1	-0.5%	4215.0	53.0	1.3%
	3p _{3/2}	3458.5	-83.5	-2.4%	3516.0	-26.0	-0.7%	†3542	3510.0	-32.0	-0.9%	3582.1	40.1	1.1%
	3d _{3/2}	2961.7	-57.3	-1.9%	3037.2	18.2	0.6%	†3019	3037.2	18.2	0.6%	3064.0	45.0	1.5%
Rn	3d _{5/2}	2830.7	-59.3	-2.1%	2906.2	16.2	0.6%	†2890	2904.0	14.0	0.5%	2930.8	40.8	1.4%
	4s	1041.6	-54.4	-5.0%	1120.5	24.5	2.2%	†1096	1120.1	24.1	2.2%	1120.1	24.1	2.2%
	4p _{1/2}	909.5	-41.5	-4.4%	954.2	3.2	0.3%	†951	957.4	6.4	0.7%	980.1	29.1	3.1%
He	4p _{3/2}	753.9	-44.1	-5.5%	798.5	0.5	0.1%	†798	796.4	-1.6	-0.2%	819.1	21.1	2.6%
	4d _{3/2}	535.0	-32.0	-5.6%	574.3	7.3	1.3%	†567	575.0	8.0	1.4%	586.6	19.6	3.5%
	4d _{5/2}	505.7	-32.3	-6.0%	545.0	7.0	1.3%	†538	544.2	6.2	1.1%	555.8	17.8	3.3%
Ne	4f _{5/2}	219.5	-22.5	-9.3%	235.3	-6.7	-2.8%	†242	235.2	-6.8	-2.8%	249.9	7.9	3.2%
	4f _{7/2}	212.5	-22.5	-9.6%	228.2	-6.8	-2.9%	†235	228.0	-7.0	-3.0%	242.7	7.7	3.3%
	5s	199.7	-12.3	-5.8%	215.0	3.0	1.4%	†212	215.2	3.2	1.5%	228.0	16.0	7.6%
Ar	5p _{1/2}	151.3	-15.7	-9.4%	168.4	1.4	0.8%	†167	169.2	2.2	1.3%	174.3	7.3	4.3%

TABLE III. (*Continued.*)

Atom	Orbital	PBE: E	ΔE	$\Delta E/E$	GW@PBE: E	ΔE	$\Delta E/E$	Expt.: E	GW@HF: E	ΔE	$\Delta E/E$	HF: E	ΔE	$\Delta E/E$
	$5p_{3/2}$	118.9	-15.1	-11.3%	136.0	2.0	1.5%	†134	135.7	1.7	1.3%	140.9	6.9	5.1%
	$5d_{3/2}$	48.7	-6.3	-11.5%	56.1	1.1	2.1%	†55	56.7	1.7	3.1%	59.7	4.7	8.6%
	$5d_{5/2}$	44.2	-6.8	-13.3%	51.7	0.7	1.3%	†51	51.9	0.9	1.7%	54.9	3.9	7.6%
	$6s$	21.5	-2.5	-10.3%	26.1	2.1	8.7%	†24	26.2	2.2	9.1%	29.0	5.0	20.8%
	$6p_{1/2}$	10.2	-3.8	-26.9%	13.7	-0.3	-2.1%	†14	14.3	0.3	2.2%	14.6	0.6	4.4%
	$6p_{3/2}$	6.7	-4.0	-37.0%	10.2	-0.5	-4.6%	†10.7	10.1	-0.6	-5.6%	10.4	-0.3	-2.6%

valence and conduction levels is too pretentious in core electron binding energies whose magnitude can be five orders of magnitude larger. With this key to understanding, the results we obtained on noble-gas atoms by the GW approximation are in very good agreement with the experiment. Indeed, GW errors on the shallowest valence electrons are always within a few tenths of eV, as usually found for GW in both chemistry and solid-state physics. At the same time, GW errors are often below 1% in deep core levels. The improvement from HF and PBE is quantified in Table II, which presents statistical averages over all energies from He to Xe. Both the MAE and the MAPE are strongly reduced when passing from either PBE or HF to GW . Most importantly, the GW self-energy contains the right and valid physics since it is able to both reduce the PBE underestimation and also the HF overestimation, in both directions. The present results represent a surprising confirmation of the GW approximation whose validity is thus verified even at high energies, tens of keV.

Last but not least, GW is surprisingly accurate on the d electrons, but also on the f . We first notice that, among all levels, d and f electrons are those where the $GW@PBE$ and $GW@HF$ values are the closest in energy, indicating that the PBE and HF wave functions are very close. This is very surprising for levels where exchange and correlation are supposed to play a major role. The GW quasiparticle renormalization factor is $Z = 0.87 \pm 0.03$ on the full set of d and f electrons, except Xe $4d$ where $Z = 0.61$. Furthermore, the shallowest d electrons (Kr $3d$, Xe $4d$, and Rn $5d$, see Fig. 2) are also the levels where GW achieves one of the best agreements with the experiment in absolute values, whereas on the deepest the relative error is at 0.5% for Rn (and also Xe) $3d$ and rises to 1.3% in Rn $4d$. On Rn $4f$ electrons GW correlations correct the HF 3.3% overestimation, but with an overshoot, at the end achieving a -2.9% underestimation. We can conclude that GW describes quite well the d -electron correlations and slightly overestimates the f -electron correlation energy.

In general, the largest errors are found at the level of the outermost s electrons (e.g., Rn $6s$, Xe $5s$, or Kr $4s$) due to difficult convergence in the GW iterations. Another source of discrepancy is the fact that our GW is not fully self-consistent

and it is self-consistent only on energies. The order of this error can be estimated from the difference between $GW@PBE$ and $GW@HF$ energies which presents also some variability along with the table. Smaller than this is the error due to the cutoff on GW parameters (number of unoccupied states in the calculation for W and Σ) and on the basis set. The order of the error due to the relativistic approximation can be estimated by comparing the two relativistic approaches considered here, ZORA and DK3 (see Supplemental Material [41] for full DK3 results). However, all Pauli spinor lowest-order v/c relativistic developments are expected to break down at large Z where also antimatter negative energies enter into play and one should solve the full relativistic Dirac equation. Furthermore, beyond the single-particle approximation considered in this Letter, *many-particle* relativistic effects should be taken into account, e.g., the Breit interaction, spin-of-one-electron orbit-of-another-electron, orbit-orbit, spin-spin, etc. [57]. These effects are very difficult to include but should be of the same order as the single-particle spin orbit. Nuclear finite mass effects, i.e., the reduced mass of electrons and the mass polarization term, are also here neglected but present well in the experiment, although the recoil energy of the final ion out of the XPS experiment has already been removed to provide corrected binding energies [2]. Finally, the experiment also contains quantum electrodynamics (QED) radiative corrections, but these do not grow with Z . The discrepancy due to the GW approximation itself, that is, the neglect of vertex corrections in the many-body self-energy and in the polarizability, is residual once eliminating all previous sources of error.

Conclusions. We benchmarked the GW approximation at high energies ($\sim 10^5$ eV) with respect to the core and valence electron removal energies. GW is in very good agreement with XPS binding energies, with a mean relative error of 1.2%. The largest discrepancies are observed at the level of the outermost s levels, whereas correlations in d and even in f electrons are surprisingly well described by GW .

Acknowledgments. We thank X. Blase and I. Duchemin for useful discussions. Parts of the calculations were done using the allocation of computational resources from GENCI-IDRIS (Grant No. 2021-A0110912036).

- [1] R. Martin, L. Reining, and D. M. Ceperley, *Interacting Electrons* (Cambridge University Press, Cambridge, UK, 2016).
[2] K. Sieghban, *ESCA Applied to Free Molecules* (North-Holland, Amsterdam, 1969).

- [3] T. A. Carlson, *Photoelectron and Auger Spectroscopy* (Plenum, New York, 1975).
[4] A. L. Fetter and J. D. Walecka, *Quantum Theory of Many-Particle Systems* (McGraw-Hill, New York, 1971).

- [5] J. Li, M. Holzmann, I. Duchemin, X. Blase, and V. Olevano, *Phys. Rev. Lett.* **118**, 163001 (2017).
- [6] J. Li, N. D. Drummond, P. Schuck, and V. Olevano, *SciPost Phys.* **6**, 040 (2019).
- [7] P. Hohenberg and W. Kohn, *Phys. Rev.* **136**, B864 (1964).
- [8] W. Kohn and L. J. Sham, *Phys. Rev.* **140**, A1133 (1965).
- [9] R. O. Jones and O. Gunnarsson, *Rev. Mod. Phys.* **61**, 689 (1989).
- [10] R. Martin, *Electronic Structure* (Cambridge University Press, Cambridge, UK, 2004).
- [11] O. Gunnarsson and B. I. Lundqvist, *Phys. Rev. B* **13**, 4274 (1976).
- [12] D. C. Langreth and M. J. Mehl, *Phys. Rev. B* **28**, 1809 (1983).
- [13] J. P. Perdew, K. Burke, and M. Ernzerhof, *Phys. Rev. Lett.* **77**, 3865 (1996).
- [14] N. Pueyo Bellafont, G. Álvarez Saiz, F. Viñes, and F. Illas, *Theor. Chem. Acc.* **135**, 35 (2016).
- [15] D. Golze, J. Wilhelm, M. J. van Setten, and P. Rinke, *J. Chem. Theory Comput.* **14**, 4856 (2018).
- [16] J. P. Perdew, R. G. Parr, M. Levy, and J. L. Balduz, *Phys. Rev. Lett.* **49**, 1691 (1982).
- [17] M. Levy, J. P. Perdew, and V. Sahni, *Phys. Rev. A* **30**, 2745 (1984).
- [18] C.-O. Almbladh and U. von Barth, *Phys. Rev. B* **31**, 3231 (1985).
- [19] L. Hedin, *Phys. Rev.* **139**, A796 (1965).
- [20] G. Strinati, H. J. Mattausch, and W. Hanke, *Phys. Rev. Lett.* **45**, 290 (1980).
- [21] G. Strinati, H. J. Mattausch, and W. Hanke, *Phys. Rev. B* **25**, 2867 (1982).
- [22] M. S. Hybertsen and S. G. Louie, *Phys. Rev. Lett.* **55**, 1418 (1985).
- [23] R. W. Godby, M. Schlüter, and L. J. Sham, *Phys. Rev. B* **35**, 4170 (1987).
- [24] L. Hedin, *J. Phys.: Condens. Matter* **11**, R489 (1999).
- [25] J. Li, I. Duchemin, O. M. Roscioni, P. Friederich, M. Anderson, E. Da Como, G. Kociok-Köhn, W. Wenzel, C. Zannoni, D. Beljonne, X. Blase, and G. D'Avino, *Mater. Horiz.* **6**, 107 (2019).
- [26] F. Bruneval, *J. Chem. Phys.* **136**, 194107 (2012).
- [27] M. J. van Setten, F. Caruso, S. Sharifzadeh, X. Ren, M. Scheffler, F. Liu, J. Lischner, L. Lin, J. R. Deslippe, S. G. Louie, C. Yang, F. Weigend, J. B. Neaton, F. Evers, and P. Rinke, *J. Chem. Theory Comput.* **11**, 5665 (2015).
- [28] E. L. Shirley and R. M. Martin, *Phys. Rev. B* **47**, 15404 (1993).
- [29] E. L. Shirley and R. M. Martin, *Phys. Rev. B* **47**, 15413 (1993).
- [30] E. L. Shirley, L. Mitáš, and R. M. Martin, *Phys. Rev. B* **44**, 3395 (1991).
- [31] S. Ishii, S. Iwata, and K. Ohno, *Mater. Trans.* **51**, 2150 (2010).
- [32] T. Aoki and K. Ohno, *J. Phys.: Condens. Matter* **30**, 21LT01 (2018).
- [33] V. K. Voora, R. Galhenage, J. C. Hemminger, and F. Furche, *J. Chem. Phys.* **151**, 134106 (2019).
- [34] M. J. van Setten, R. Costa, F. Viñes, and F. Illas, *J. Chem. Theory Comput.* **14**, 877 (2018).
- [35] D. Golze, L. Keller, and P. Rinke, *J. Phys. Chem. Lett.* **11**, 1840 (2020).
- [36] C. Chang, M. Pélissier, and P. Durand, *Phys. Scr.* **34**, 394 (1986).
- [37] J.-L. Heully, I. Lindgren, E. Lindroth, S. Lundqvist, and A.-M. Martensson-Pendrill, *J. Phys. B* **19**, 2799 (1986).
- [38] E. van Lenthe, E. J. Baerends, and J. G. Snijders, *J. Chem. Phys.* **99**, 4597 (1993).
- [39] T. Nakajima and K. Hirao, *Chem. Phys. Lett.* **329**, 511 (2000).
- [40] T. Nakajima and K. Hirao, *J. Chem. Phys.* **113**, 7786 (2000).
- [41] See Supplemental Material at <http://link.aps.org/supplemental/10.1103/PhysRevB.106.L081125> for DK3 results and machine readable tables.
- [42] W. Lotz, *J. Opt. Soc. Am.* **60**, 206 (1970).
- [43] N. Marom, F. Caruso, X. Ren, O. T. Hofmann, T. Körzdörfer, J. R. Chelikowsky, A. Rubio, M. Scheffler, and P. Rinke, *Phys. Rev. B* **86**, 245127 (2012).
- [44] P. Pollak and F. Weigend, *J. Chem. Theory Comput.* **13**, 3696 (2017).
- [45] I. Duchemin, J. Li, and X. Blase, *J. Chem. Theory Comput.* **13**, 1199 (2017).
- [46] F. Weigend, *J. Comput. Chem.* **29**, 167 (2008).
- [47] G. L. Stoychev, A. A. Auer, and F. Neese, *J. Chem. Theory Comput.* **13**, 554 (2017).
- [48] M. Valiev, E. Bylaska, N. Govind, K. Kowalski, T. Straatsma, H. V. Dam, D. Wang, J. Nieplocha, E. Apra, T. Windus, and W. de Jong, *Comput. Phys. Commun.* **181**, 1477 (2010).
- [49] X. Blase, C. Attaccalite, and V. Olevano, *Phys. Rev. B* **83**, 115103 (2011).
- [50] D. Jacquemin, I. Duchemin, and X. Blase, *J. Chem. Theory Comput.* **11**, 3290 (2015).
- [51] J. Li, G. D'Avino, I. Duchemin, D. Beljonne, and X. Blase, *J. Phys. Chem. Lett.* **7**, 2814 (2016).
- [52] S. G. Balasubramani, G. P. Chen, S. Coriani, M. Diedenhofen, M. S. Frank, Y. J. Franzke, F. Furche, R. Grotjahn, M. E. Harding, C. Hättig, A. Hellweg, B. Helmich-Paris, C. Holzer, U. Huniar, M. Kaupp, A. Marefat Khah, S. Karbalaee Khani, T. Müller, F. Mack, B. D. Nguyen *et al.*, *J. Chem. Phys.* **152**, 184107 (2020).
- [53] *X-ray Data Booklet*, edited by A. Thompson (Lawrence Berkeley National Laboratory, Berkeley, CA, 2009).
- [54] J. A. Bearden and A. F. Burr, *Rev. Mod. Phys.* **39**, 125 (1967).
- [55] M. G. Pia, H. Seo, M. Batic, M. Begalli, C. H. Kim, L. Quintieri, and P. Saracco, *IEEE Trans. Nucl. Sci.* **58**, 3246 (2011).
- [56] V. Atalla, M. Yoon, F. Caruso, P. Rinke, and M. Scheffler, *Phys. Rev. B* **88**, 165122 (2013).
- [57] V. Olevano and M. Ladisa, [arXiv:1002.2117](https://arxiv.org/abs/1002.2117).